

# Gelation Kinetics and Mechanical Properties of Thiol-Tetrazole Methylsulfone Hydrogels Designed for Cell Encapsulation

Adrián de Miguel-Jiménez, Bastian Ebeling, Julieta I. Paez, Claudia Fink-Straube, Samuel Pearson,\* and Aránzazu del Campo\*

Hydrogel precursors that crosslink within minutes are essential for the development of cell encapsulation matrices and their implementation in automated systems. Such timescales allow sufficient mixing of cells and hydrogel precursors under low shear forces and the achievement of homogeneous networks and cell distributions in the 3D cell culture. The previous work showed that the thiol-tetrazole methylsulfone (TzMS) reaction crosslinks star-poly(ethylene glycol) (PEG) hydrogels within minutes at around physiological pH and can be accelerated or slowed down with small pH changes. The resulting hydrogels are cytocompatible and stable in cell culture conditions. Here, the gelation kinetics and mechanical properties of PEG-based hydrogels formed by thiol-TzMS crosslinking as a function of buffer, crosslinker structure and degree of TzMS functionality are reported. Crosslinkers of different architecture, length and chemical nature (PEG versus peptide) are tested, and degree of TzMS functionality is modified by inclusion of RGD cell-adhesive ligand, all at concentration ranges typically used in cell culture. These studies corroborate that thiol/PEG-4TzMS hydrogels show gelation times and stiffnesses that are suitable for 3D cell encapsulation and tunable through changes in hydrogel composition. The results of this study guide formulation of encapsulating hydrogels for manual and automated 3D cell culture.

## 1. Introduction


Hydrogels have broad use as biomaterials, ranging from scaffolds for fundamental cell studies to translational products in sprayable, injectable, and implantable formats.<sup>[1]</sup> They are particularly appealing for generating cell-laden constructs as 3D cultures or cell-based therapeutic products. Crosslinking of liquid precursors is performed in the presence of the cells, and the networks can be designed with features that emulate the native extracellular environment.<sup>[2]</sup> Hydrogel matrices that allow reliable and automatable 3D cell encapsulation are important in these contexts.

The properties of the crosslinking reaction are fundamental for successful 3D cell encapsulation. The reaction needs to i) work at near-physiological conditions, ii) proceed at a rate that permits complete mixing and homogeneous cell suspension, iii) reach completion in the presence of other reactive groups in the biological milieu, iv) form linkages that are stable over a desired timescale, and v) be cytocompatible. To reach widespread adoption, the

pre-polymers bearing the crosslinkable groups should also be easily attained and stable in storage.

A. de Miguel-Jiménez, J. I. Paez, C. Fink-Straube, S. Pearson, A. del Campo  
INM – Leibniz Institute for New Materials  
Campus D2 2, 66123 Saarbrücken, Germany  
E-mail: samuel.pearson@leibniz-inm.de;  
aranzazu.delcampo@leibniz-inm.de

A. de Miguel-Jiménez, A. del Campo  
Chemistry Department  
Saarland University  
66123 Saarbrücken, Germany  
B. Ebeling  
Kuraray Europe GmbH  
Advanced Interlayer Solutions  
Competence Center for Innovation & Technology  
Mülheimer Str. 26, 53840 Troisdorf, Germany  
J. I. Paez  
Current address: Department of Developmental BioEngineering  
Technical Medical Centre  
University of Twente  
Enschede The Netherlands

 The ORCID identification number(s) for the author(s) of this article can be found under <https://doi.org/10.1002/mabi.202200419>

© 2022 The Authors. Macromolecular Bioscience published by Wiley-VCH GmbH. This is an open access article under the terms of the Creative Commons Attribution-NonCommercial License, which permits use, distribution and reproduction in any medium, provided the original work is properly cited and is not used for commercial purposes.

DOI: 10.1002/mabi.202200419

We recently demonstrated that thiol-methylsulfone (MS) coupling chemistry is promising for 3D cell encapsulation, with starPEG-based derivatives meeting all the above criteria and thereby surpassing some of the limitations of the commonly used thiol/maleimide (Mal) and thiol/vinylsulfone (VS) crosslinking systems.<sup>[3,4]</sup> The three tested MS candidates – oxadiazole (OxMS), tetrazole (TzMS) and benzothiazole (BtMS) – reliably formed hydrogels that were cytocompatible, with L929 fibroblasts demonstrating >92% viability after 7 days culture.<sup>[4]</sup> Encapsulated fibroblast spheroids showed cell spreading and active migration indicating both recognition of cell-adhesive RGD ligands and degradation of the matrix metalloproteinase (MMP)-cleavable peptidic bonds provided by the VPM crosslinker.<sup>[3]</sup> More sensitive human umbilical vein endothelial cells demonstrated >94% viability after 1 day,<sup>[3]</sup> showing comparable cytocompatibility to other prevalent PEG-based gelation systems.<sup>[5]</sup> Thiol/MS crosslinking of PEG-based gels therefore proved suitable for various 3D cell encapsulation scenarios on the basis of cell viability, morphogenesis, and migration studies. The three MS candidates showed differences in gelation rate, stability in long-term cell culture, and ease and cost of synthesis, with the TzMS derivative emerging as the leading option across all of these metrics. PEG-4TzMS gels formed on a minutes timescale at pH 7.5.<sup>[4]</sup> The thiol-TzMS gels were the most stable of the three derivatives, enduring for 15 days under cell culture conditions.<sup>[4]</sup> The TzMS-derivatized PEG polymers could also be synthesized cheaply on gram scale, and showed excellent stability in storage and in aqueous solution.

The rheological study of crosslinking kinetics and mechanical properties of PEG-4TzMS was performed on hydrogels with 20 kDa PEG-4SH as a model crosslinker.<sup>[4]</sup> However, in cell encapsulation and culture studies precursors need to be pre-functionalized with adhesive ligands and crosslinked with degradable peptides of different length and functionality, which influence the gelation kinetics and final properties of the hydrogel. These parameters are adjusted in cell cultures to meet the needs of individual cell types, and their impact in the gelation process and the network properties are important to understand.<sup>[6]</sup> Recent studies highlight the implications of gelation rate in the local gel homogeneity, and its consequences for the mechanics of the network and reproducibility of the final cell experiments.<sup>[7]</sup> Along this line, the present work compares the gelation kinetics and final mechanical properties of PEG-4TzMS-based hydrogels using PEG-4SH, linear PEG-dithiols and VPM as crosslinkers, and with incorporation of cell-adhesive ligand RGD prior to crosslinking. Different pH and buffering conditions are explored as additional handles to control the gelation process. We aim to facilitate the establishment of cell culture models based on PEG-TzMS hydrogels by illustrating how compositional changes might impact the quality and properties of the final networks.

## 2. Results

Hydrogels in this work are based on 20 kDa 4-arm starPEG end-functionalized with TzMS groups at degrees of functionalization, denoted  $F_{TzMS}$ , of >95%.<sup>[3]</sup> Crosslinking was achieved with PEG-4SH (20 kDa) or dithiols of different molar masses and either PEG or peptidic backbones. For each crosslinker, the degree

of thiol functionalization is represented by  $F_{SH}$ . For the rheology measurements, PEG-4TzMS and thiol solutions in the corresponding buffer were mixed directly on the rheometer plate at 25 °C, and the evolution of shear storage ( $G'$ ) and loss ( $G''$ ) moduli was monitored throughout crosslinking. The addition sequence, volume, and mixing protocol are important for reproducibility and are detailed in the experimental section. All rheology curves start at 1 min, which was the time needed for mixing of the gel precursor solution and launch of the instrument. To compare crosslinking kinetics among the different formulations, we selected the time required for  $G' > 50$  Pa (denoted  $t_{50Pa}$ ) as a proxy for the gelation onset, since the conventionally used<sup>[8]</sup> crossover of  $G'$  and  $G''$  was not always observed. The value of  $G'$  at minute 40 ( $G'_{40min}$ ) was taken as a measure of the crosslinking degree achieved at different pH values within a given formulation, and for comparing the stiffness across the different hydrogel formulations.

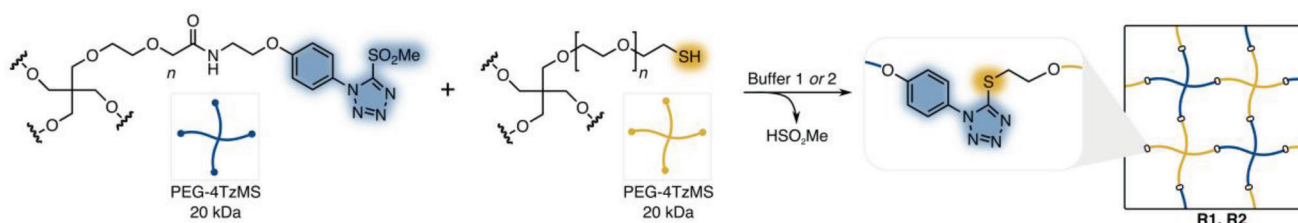
All experiments in our study were performed keeping the total polymer content in the hydrogels at 5.0% w/v. This is a typical polymer concentration used for cell encapsulation with 20 kDa starPEGs.<sup>[3,5,6]</sup> The concentration of the individual precursors was fixed such that  $[SH]:[MS] = 1:1$ . The exact stoichiometry was calculated for each polymer batch considering the degree of functionalization and the molar mass from <sup>1</sup>H NMR analysis of the PEG precursors (Figures S1 and S2 and Table S1, Supporting Information) or the purity degree from HPLC analysis in the case of the peptide reactants (Table S2, Supporting Information). We anticipate that this procedure leads to hydrogels with higher  $G'$  values than when using the molar mass and end group determination taken from the suppliers' material data sheets for the calculation.<sup>[4]</sup> An exact 1:1 ratio of reactive groups should lead to more complete crosslinking and fewer network defects.<sup>[9]</sup>

### 2.1. The Importance of Buffer Selection

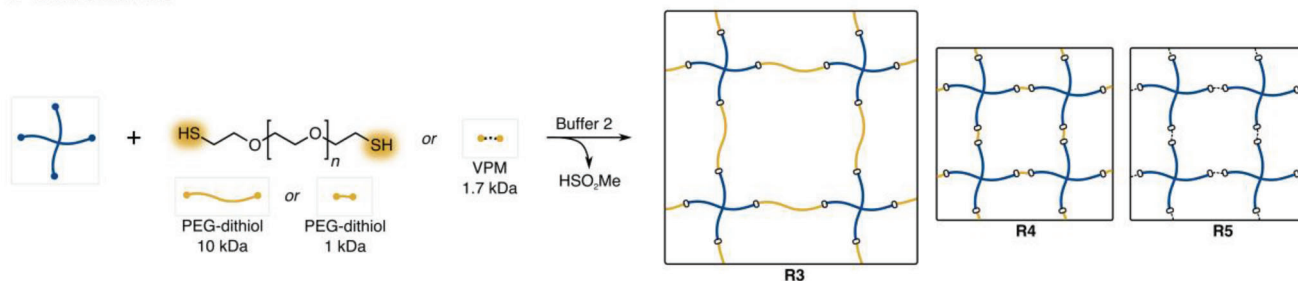
The thiol-MS reaction is sensitive to pH in two ways (**Scheme 1**). First, the initial pH of the medium affects the concentration of the nucleophilic thiolate as reactive intermediate. Higher initial reaction rates are therefore expected at higher pH values. Second, the methanesulfinic acid byproduct of the thiol-MS reaction can lead to a progressive decline in pH value during the reaction if the proton concentration exceeds the buffering capacity of the medium. This can slow down the reaction and reduce the conversion (i.e., crosslinking) degree.<sup>[3]</sup> We therefore first tested the pH progression during gelation in our working conditions and searched for a buffer system that could maintain a stable pH.

In our experiments, precursor solutions were prepared at the target pH values. Initial experiments were performed by crosslinking PEG-4TzMS with PEG-4SH in 10 mM HEPES buffer at pH 8.0, 7.5, and 7.0 (**R1, Table 1**). In these conditions, we observed lower initial gelation rate and less stiff gels at lower initial pH values (**Figure 1A**), as reflected in the higher  $t_{50Pa}$  and lower  $G'_{40min}$  values (Table 1). pH monitoring of separate solutions with the same compositions as the rheology experiments showed a sharp decline in the pH of the reaction mixtures within 1 min of mixing, followed by a slower decline over the remainder of the 40 min measurement time (Figure 1A). Over the 40 min reaction time, decreases of >1.6 pH units in the pH 7.0 system,

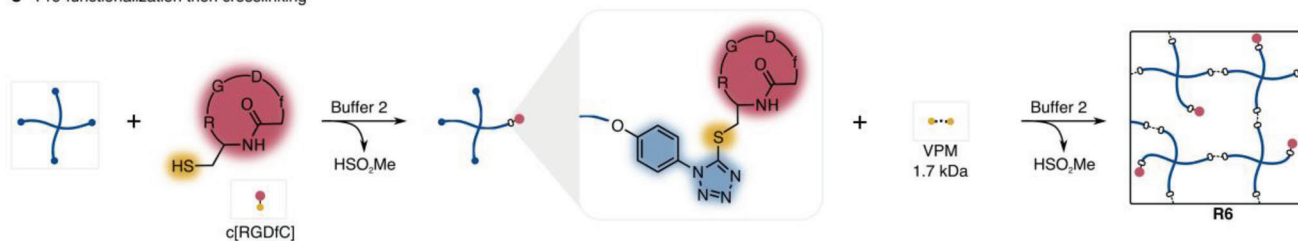
**A** StarPEG crosslinker



**B** Linear crosslinkers



**C** Pre-functionalization then crosslinking



**Scheme 1.** Overview of representative networks formed by PEG-4TzMS reaction with A) PEG-4SH, B) Linear crosslinkers PEG-dithiol (10 and 1 kDa) and VPM, and C) c[RGDFC] as a prefunctionalization step before reaction with VPM. **R1–R6** refer to the rheology experiments in Table 1. Buffer 1 = 10 mM HEPES, Buffer 2 = 20 mM HEPES + 40 mM sodium bicarbonate, VPM = GCRDVPMSMRGGDRCG peptide.

0.9 pH units in the pH 7.5 system, and 0.8 pH units in the pH 8.0 system were observed. These results indicate that at the reactive group concentrations used in **R1**, the buffering capacity of 10 mM HEPES was insufficient to combat the generated methanesulfinic acid and maintain stable pH values. The expected trend of slower gelation at lower initial pH values is therefore amplified by the subsequent drops in pH value, which were more dramatic at lower initial pH values since pH declines significantly below the optimum buffering range for HEPES ( $pK_a \approx 7.6$ ).<sup>[10]</sup> The slow reaction at pH 7.0 meant  $t_{50Pa}$  exceeded 10 min, and the  $G'_{40min}$  of just 650 Pa shows that the crosslinking degree in this system was far inferior to those at higher pH values, due to the combined effects of low initial pH and declining pH as crosslinking proceeded.

To maintain a stable pH during crosslinking, we adopted a buffering system containing 20 mM HEPES and 40 mM sodium bicarbonate. Bicarbonate buffers are the most prevalent for cell culture, and concentrations from 22 mM (i.e., physiological concentration) to 44 mM are standard.<sup>[11]</sup> HEPES concentrations up to 25 mM are typically included in 3D cell culture medium to provide additional buffering capacity to bicarbonate. The buffer concentrations in this work are therefore within cytocompat-

ble ranges. During the gelation of PEG-4TzMS and PEG-4SH using this buffer (**R2**, Table 1) considerably smaller pH drops of <0.3 pH units were observed (Figure 1B). At a given initial pH value,  $t_{50Pa}$  was shorter and  $G'_{40min}$  was higher than in experiments using 10 mM HEPES (**R1**). At pH 7.0 for example,  $t_{50Pa}$  decreased from 11.1 (**R1**) to 3.0 min (**R2**), and  $G'_{40min}$  increased from 660 to 5590 Pa. These results confirm that the slower kinetics and lower conversions at lower initial pH values in **R1** are a result of declining pH value throughout crosslinking. Interestingly, higher values of  $G'_{40min}$  were obtained with decreasing pH value in **R2**;  $G'_{40min}$  was 3560 Pa at pH 8.0, 4690 Pa at pH 7.5, and 5590 Pa at pH 7.0. In line with previous work, we hypothesize that the slower crosslinking rate at lower pH leads to formation of a more homogeneous and complete network that achieves higher stiffness values by limiting the extent to which the reaction proceeds during the mixing phase wherein the reactive partners are inhomogeneously distributed.<sup>[3]</sup> In contrast,  $G'_{40min}$  in **R1** was lowest at pH 7.0 because this system exhibited the greatest decline in pH value and the reaction became prohibitively slow. The 20 mM HEPES and 40 mM sodium bicarbonate buffer was used for the remaining experiments in this paper.

**Table 1.** Experimental parameters and results of the rheology experiments performed in this work.

# <sup>a)</sup>	PEG-4TzMS [% w/v]	c[RGDfC] [mM]	$F_{TzMS,final}$ [%] <sup>b)</sup>	[MS] <sub>final</sub> [mM]	Crosslinker [% w/v]	[SH] <sub>theor</sub> <sup>c)</sup> [mM]	[SH]:[MS] <sub>theor</sub>	[P] <sub>total</sub> [% w/v]	Buffer <sup>d)</sup>	pH <sub>initial</sub>	$t_{50Pa}$ [min] <sup>e)</sup>	$G'_{40min}$ [Pa]
<b>R1</b>	2.55	-	98.3	4.40	20 kDa PEG-4SH 2.49	4.48	1.02	5.04	1	8.0	1.2 ± 0.1	4208 ± 480
										7.5	2.9 ± 0.1	3694 ± 140
										7.0	11.1 ± 0.4	650 ± 29
<b>R2</b>	2.54	-	96.4	4.39	20 kDa PEG-4SH 2.49	4.39	1.00	5.03	2	8.0	<1	3560 ± 895
										7.5	1.2 ± 0.2	4685 ± 692
										7.0	3.0 ± 0.3	5590 ± 937
<b>R3</b>	2.37	-	96.4	4.24	10 kDa PEG-dithiol 2.66	4.24	1.00	5.03	2	8.0	2.2 ± 0.2	1013 ± 289
										7.5	3.8 ± 0.1	967 ± 146
<b>R4</b>	4.50	-	96.4	8.14	1 kDa PEG-dithiol 0.56	8.14	1.00	5.06	2	8.0	<1	2422 ± 161
										7.5	1.8 ± 0.1	3080 ± 486
<b>R5</b>	4.43	-	96.4	7.74	VPM 0.65	7.74	1.00	5.08	2	8.0	<1	840 ± 233
										7.5	1.6 ± 0.2	1149 ± 348
<b>R6</b>	4.46	1.29	83.3 <sup>f)</sup>	6.55	VPM 0.54	6.20	0.95	4.98 <sup>g)</sup>	2	8.0	<1	321 ± 94
										7.5	4.1 ± 0.9	272 ± 125
										7.0	6.3 ± 1.1	243 ± 147

<sup>a)</sup> Rheometer settings:  $T = 25\text{ }^{\circ}\text{C}$ ,  $V_{total} = 36.0\text{ }\mu\text{L}$ ,  $gap = 300\text{ }\mu\text{m}$ ,  $strain = 1\%$ ,  $frequency = 1\text{ Hz}$ ; <sup>b)</sup>  $F_{TzMS,final}$  = degree of functionality of the starPEG immediately prior to crosslinking, i.e., the percentage of end groups that bear the TzMS function; <sup>c)</sup> This theoretical value is the expected thiol content of the crosslinkers based on <sup>1</sup>H NMR spectroscopy (PEG-based crosslinkers) and HPLC (VPM) analyses; <sup>d)</sup> Buffer 1: 10 mM HEPES. Buffer 2: 20 mM HEPES + 40 mM sodium bicarbonate; <sup>e)</sup> Values < 1 min indicate that the  $G'$  was above 50 kPa at the 1 min timepoint; <sup>f)</sup> Value determined by <sup>1</sup>H NMR spectroscopy of isolated polymer; <sup>g)</sup> Overall mass does not consider the mass contributed by the c[RGDfC] ligand.

## 2.2. The Influence of Crosslinker Architecture and Molar Mass

Linear dithiol crosslinkers and degradable peptides terminated with cysteine residues are often used in the formulation of PEG-based hydrogels for cell culture.<sup>[12,13]</sup> We compared the gelation kinetics and the properties of PEG-4TzMS hydrogels crosslinked with linear dithiols of two different molar masses: a 10 kDa PEG-dithiol (**R3**, Table 1), which offers the same thiol content per unit mass as the PEG-4SH but without the star structure, and a 1 kDa PEG-dithiol (**R4**, Table 1) which is shorter than the 10 kDa analog, but has similar length to a typical MMP-degradable peptide crosslinker. Finally, experiments with the 1.7 kDa degradable peptide VPM bearing two cysteines (**R5**, Table 1) were also performed.

Hydrogels with 10 kDa PEG-dithiol as crosslinker (**R3**) presented longer  $t_{50Pa}$  and smaller  $G'_{40min}$  values than **R2** hydrogels crosslinked with PEG-4SH (Figure 1C, Table 1). This agrees with the lower concentration of network points (Scheme 1). Only the star PEG-4TzMS molecule, which is present at 2.4% w/v, can contribute network points after crosslinking, with the 2.6% w/v of linear 10 kDa PEG-dithiol serving only as a connector between stars. Hydrogels crosslinked with 1 kDa PEG-dithiol (**R4**) showed faster crosslinking and higher final stiffnesses than **R3** hydrogels (Figure 1D, Table 1). The molar concentration of reactive groups present in the **R4** systems was almost double that in **R3** (for a constant polymer total concentration of 5% w/v), and this translated to a faster rise in  $G'$ . The **R4** systems also had almost twice the concentration of PEG-4TzMS than the **R3** hydrogels (Table 1). The higher concentration of network points explains the higher  $G'_{40min}$  values.

During crosslinking of **R4** hydrogels at pH 8.0, an initial drop of 0.4–0.5 pH units was observed (Figure 1D). This is due to the relatively high concentration of reactive groups generating considerable amounts of methanesulfinic acid in the beginning of the crosslinking process. The initial decline in pH was less pronounced at pH 7.5, presumably due to the lower initial rate of acid generation and the better buffering ability of the HEPES component of the buffer at pH 7.5 given its pKa of  $\approx 7.6$ .<sup>[10]</sup> Hydrogels containing the peptidic dithiol crosslinker VPM (**R5**) showed similar  $t_{50Pa}$  to hydrogels crosslinked with 1 kDa PEG-dithiol (**R4**), but approximately threefold lower  $G'_{40min}$  values (Figure 1E, Table 1). The reactive group concentration, the PEG-4TzMS mass content, and the concentration of network points in **R5** are  $\approx 10\%$  lower than in **R4**, which partially explain the lower stiffness of the final hydrogel. Deviation from expected 1:1 reactive group stoichiometry in the VPM system could also lower the stiffness, and is explored in Section 2.4.

## 2.3. The Effect of Pre-Functionalization with Cell-Adhesive Ligand

To serve as artificial matrices for 3D cell culture, PEG hydrogels need to be biofunctionalized with cell-adhesive moieties such as the RGD peptide.<sup>[14,15]</sup> In our system, thiolated bioactive molecules can be incorporated into the gel network by pre-incubation with the PEG-4TzMS pre-polymer. This step consumes reactive sites, and is expected to affect  $t_{50Pa}$  and  $G'_{40min}$  values by decreasing the concentration of MS groups available for crosslinking. The higher the adhesive ligand content, the lower the reactive sites available for crosslinking.



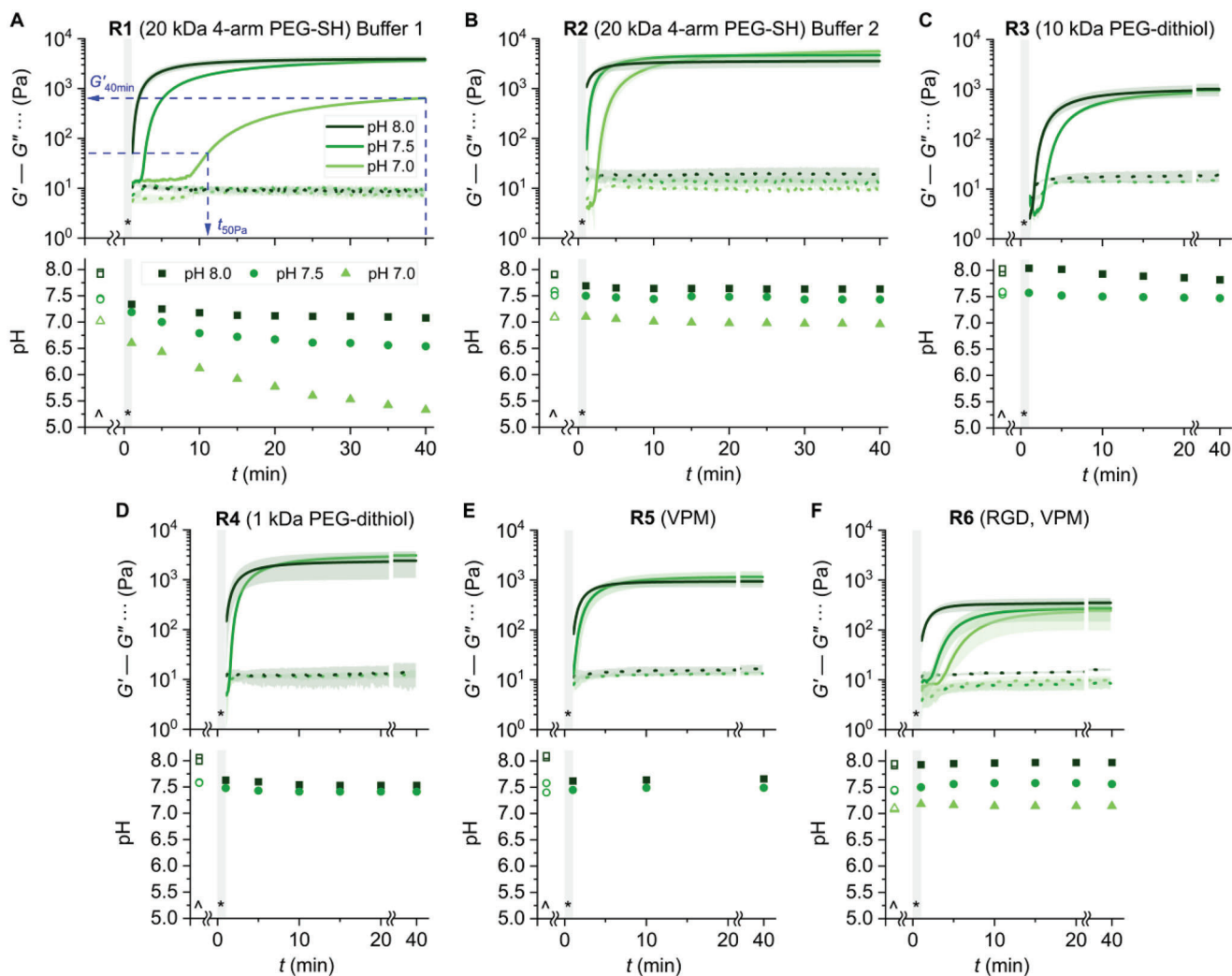


**Figure 1.** Rheology and pH monitoring during gelation of PEG-4TzMS and crosslinkers. A) **R1**, B) **R2**, C) **R3**, D) **R4**, E) **R5**, and F) **R6**, conditions in Table 1;  $N = 3$  at all pH values for rheology, except **R6** for which  $N = 4$ .  $N = 1$  for all pH tracking points. \* = time period for solution mixing and rheometer launch (60 s). ^ = time period before mixing during which pH values of precursor solutions were measured.

We explored the effect of  $c[\text{RGDfC}]$  incorporation on the gelation rate and final mechanical properties of resulting hydrogels. In the following, we express ligand content in terms of the degree of functionality of the TzMS units ( $F_{\text{TzMS}}$ ), i.e., the proportion of end groups carrying the TzMS function, since this accounts for any variability in the degree of functionality of precursor polymers. PEG-4TzMS ( $F_{\text{TzMS}} = 0.964$ ) was incubated with  $c[\text{RGDfC}]$  at a molar ratio that targeted  $F_{\text{TzMS}} = 0.80$  after complete reaction.  $^1\text{H}$  NMR spectroscopy analysis confirmed that  $c[\text{RGDfC}]$  (**Figure 2A**) was covalently attached to PEG-4TzMS (**Figure 2B**), with the aromatic proton signal “b” at 7.6 ppm shifting 0.1 ppm upfield upon thiol substitution of the MS group (**Figure 2C**). A similar shift in the 7.6 ppm proton signal upon thiol substitution was also observed for model substitutions with mercaptoethanol (data not shown). Integration of the aromatic proton signals in **Figure 2C** showed incorporation of the  $c[\text{RGDfC}]$  ligand to give  $F_{\text{TzMS}}$  of 0.83, which is slightly higher than the expected value of 0.80 and indicates that a portion of the feed  $c[\text{RGDfC}]$  ( $\approx 20\%$ ) was not incorporated into the 4-arm starPEG.

The gelation of hydrogels crosslinked with VPM after functionalization with  $c[\text{RGDfC}]$  (**R6**) was then characterized.  $t_{50\text{Pa}}$  ranged from just over 1 min at pH 8.0 to 4 min at pH 7.5 and 6 min at pH 7.0. These  $t_{50\text{Pa}}$  values are significantly longer than in the non-biofunctionalized hydrogel **R5**, in agreement with the lower number of reactive groups available for building the network. In line with this argument,  $G'_{40\text{min}}$  was also approximately threefold lower (**Table 1**), reaching 240–320 Pa across the three tested pH values. In decreasing the overall proportion of end groups with TzMS functions, the prefunctionalization step changes the distribution of PEG molecules bearing 0, 1, 2, 3, and 4 terminal TzMS groups. The expected distributions can be determined theoretically and depend on the reaction conditions for the (de)functionalization of arms. The resulting distributions were deduced for the limiting cases of diffusion and reaction control by simulations (see Supporting Information for details). **Figure 3** shows the mean distributions for both studied systems with the black vertical bars indicating the possible range defined by the limiting cases. In PEG-4TzMS ( $F_{\text{TzMS}} = 0.964$ , **Figure 3A**),

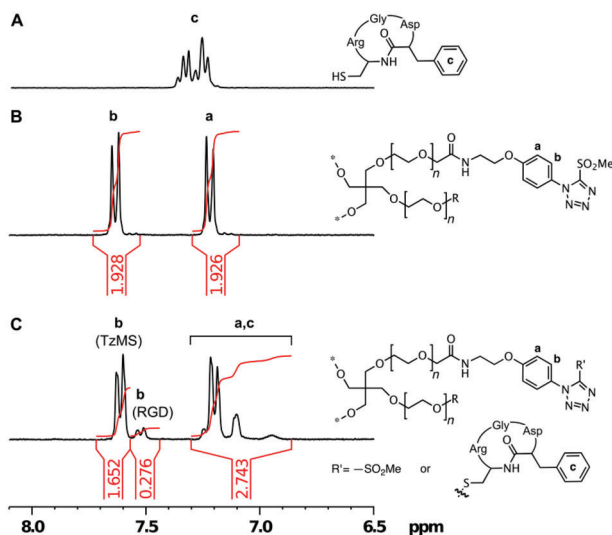


**Figure 2.**  $^1\text{H}$  NMR spectra (300 MHz,  $\text{D}_2\text{O}$ ) of A) c[RGDFc], B) PEG-4TzMS, and C) the purified polymer after reaction with c[RGDFc] to give  $F_{\text{TzMS}} = 0.83$ . Reaction conditions: pH 8.0, 20 mM HEPES with 40 mM sodium bicarbonate, 1 h reaction time.

96.4–99.3% of the stars bear 3 or 4 TzMS groups and can therefore generate network points during crosslinking. After RGD functionalization ( $F_{\text{TzMS}} = 0.833$ , Figure 3B), 13.2–15.0% of stars carry  $\leq 2$  TzMS functions. Species with 2 active arms (10.9–11.6% of stars) can act only as linear chain extenders during the crosslinking process with VPM and are not able to contribute network points, and species with only one active arm (1.6–3.1% of stars) can only be incorporated into the network as terminal units. Only the 85.0–86.7% of remaining stars (3 or 4 arms bearing TzMS) can introduce network points when reacted with VPM.

#### 2.4. Maximizing $G'_{40\text{min}}$ by Varying the Reactive Group Stoichiometry with VPM Crosslinkers

Throughout this work, a 1:1 stoichiometry between SH and MS was imposed, since consumption of all reactive partners would form the most complete network with the highest stiffness. Modest deviations from 1:1 stoichiometry in other step-growth hydrogels have been shown to significantly decrease the stiffness.<sup>[16,17]</sup> The significantly lower  $G'_{40\text{min}}$  values obtained when using VPM versus 1 kDa PEG-dithiol prompted us to check the relationship between stoichiometry and final stiffness. We analyzed **R6** systems with variable [SH]:[MS] ratio from 0.93 up to 1.31 at pH 7.0 by preparing identical stock solutions to those used for previous rheology experiments (Figure 1) and adding different volume ratios of the two solutions to the rheometer. An increase in  $G'_{40\text{min}}$  was observed with increasing VPM concentration, reaching a fourfold higher  $G'_{40\text{min}}$  value at 17% excess VPM (Figure 4A) compared to 1:1 stoichiometry. A similar study performed on the **R5** system at pH 8.0 showed a peak in  $G'_{40\text{min}}$  at 40% excess VPM (Figure 4B). Note that these experiments were performed by starting with identical stock solutions of the starPEG and crosslinker, and adding these solutions in different volume ratios to the rheometer plate. At [SH]:[MS] ratios above 1, the total polymer concentration (5.0% w/v at 1:1 stoichiometry) declines,

reaching 4.3% w/v at [SH]:[MS] = 1.4. The higher  $G'_{40\text{min}}$  values observed at excess VPM were therefore obtained despite slightly lower overall polymer contents. The results confirm that a significantly higher ratio of VPM to MS groups is required to maximize hydrogel stiffness. In contrast, hydrogels crosslinked with PEG-dithiol crosslinkers (**R3** and **R4** systems) showed a maximum  $G'_{40\text{min}}$  at [SH]:[MS] = 1 (Figure 4C; Figure S3, Supporting Information), and excess dithiol resulted in hydrogels with significantly lower stiffness. The increase in stiffness at excess VPM contents suggests that a competing reaction such as disulfide formation could be decreasing the availability of crosslinking (thiol) functions.

We checked disulfide bond formation in commercial VPM by using liquid chromatography/electrospray ionization quadrupole time-of-flight mass spectrometry (LC/ESI QTOF-MS). A VPM stock solution with identical composition to the precursor solution at pH 8.0 in **R5** was used for this experiment. According to the detected  $m/z$  values, three main species were detected from the beginning of the experiment: VPM, linear VPM dimer and cyclic VPM species (Figure S4, Supporting Information). VPM in its 3+ state was the dominant component. The preference for the 3+ state arises from the three arginine residues in the structure that are protonated at the tested pH value. The cyclic VPM species containing disulfide(s) and zero available thiols could be unimeric, dimeric, (etc.) since these would exhibit the same  $m/z$  value. Differentiation of these species would require a more elaborate LC protocol to separate them chromatographically prior to mass spectrometry analysis. The proportion of thiols locked up in disulfides was calculated from the counts (Figure S5, Supporting Information) since detector counts are proportional to the molar concentration of each species in solution. Initially, 2.2–5.3% of the thiol groups was in the form of disulfide bonds, and this number reached 7.2–14.2% over the next 60 min at pH 8.0 (Figure 5). The rheology experiments typically require  $\approx 10$  min between VPM solution preparation and mixing with PEG-4TzMS. The thiol concentration was therefore likely to be already 3–6% lower than theoretical values in **R5** and **R6** at the beginning of the network formation. Significant here is the fact that the linear VPM dimer is still capable of reacting with MS groups and contributing to crosslinking, since it contains a thiol at each end, while the cyclic VPM dimer cannot react with any MS groups. This ability to compensate for functional group loss by adding excess crosslinker is unique to systems where the loss occurs through coupling reactions, since monofunctional species that could only contribute dangling ends to the network are absent. The need for excess VPM to attain peak  $G'_{40\text{min}}$  values (Figure 4) can then be partially attributed to the competing disulfide reaction in the precursor solutions uptaking part of the thiols, although the required excess of VPM was higher than accounted for by disulfide formation determined here.

### 3. Discussion

On the molecular scale, 3D polymer networks are inherently heterogeneous, exhibiting dangling ends, loops, double or triple links (in star-shape polymers), and entanglements because of the stochastic cross-linking reaction processes.<sup>[18]</sup> These molecular defects result in a nonuniform distribution of polymer chains

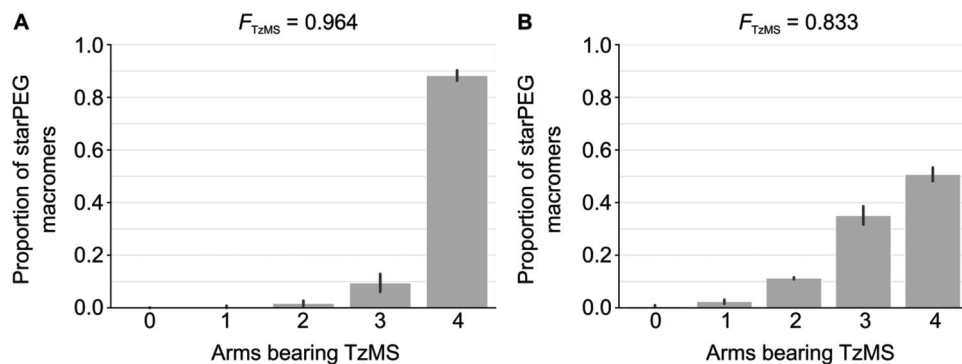


**Figure 3.** Proportion of starPEG macromers bearing 0, 1, 2, 3, and 4 TzMS groups at the chain ends for A)  $F_{TzMS} = 0.964$ , and b)  $F_{TzMS} = 0.833$  obtained by functionalization of the polymer in A) with c[RGDfC] under the limiting cases of pure diffusion- and reaction-control. The vertical bars show the range of possibly attainable values according to these two limiting cases.

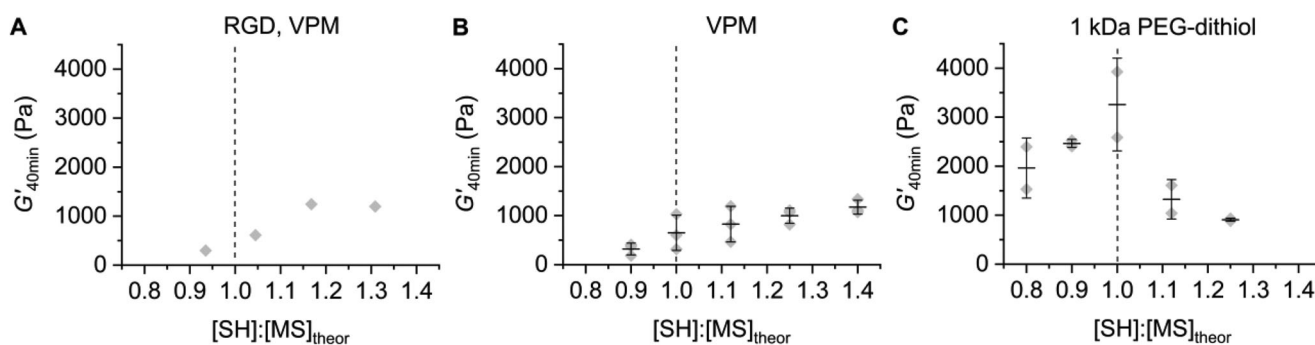


**Figure 4.** Effect of reactive group stoichiometry on  $G'_{40min}$  for A) PEG-4TzMS pre-functionalized with c[RGDfC] followed by VPM crosslinking at pH 7.0 (identical to **R6** at  $[SH]:[MS] = 0.95$ ),  $N = 1$ , B) PEG-4TzMS crosslinked with VPM at pH 8.0 (identical to **R5** at  $[SH]:[MS] = 1$ ),  $N = 3$ , and C) PEG-4TzMS crosslinked with 1 kDa PEG-dithiol at pH 8.0 (identical to **R4** at  $[SH]:[MS] = 1$ ),  $N = 2$ . The vertical dotted line shows theoretical 1:1 stoichiometry. For B) and C), the mean  $\pm$  standard deviation values are shown in addition to individual data points.

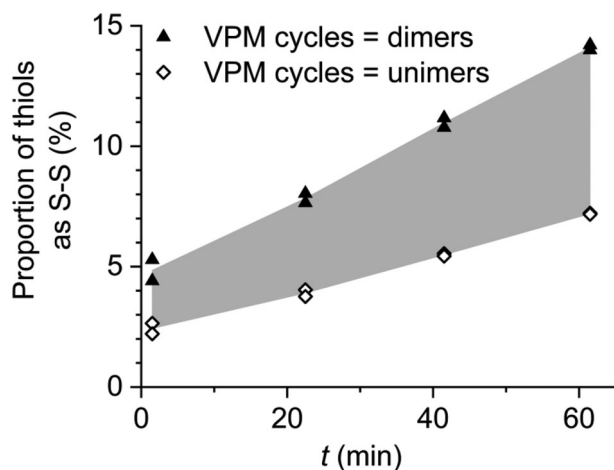


**Figure 5.** Quantification of VPM, linear VPM dimer, and cyclic VPM species (unimer or dimer) over time at pH 8.0 by LC/ESI QTOF-MS,  $N = 2$ . The composition of the solution was as used in **R5** crosslinking experiment (pH 8.0). The shaded area shows the range between the two conditions, using the average of values from each condition as boundary lines.

and, consequently, in spatial defects at different length scales. For 3D cell encapsulation, spatial defects can translate to inconsistent cell responses, since cells can experience different local

crosslinking degrees and ligand densities through the gel volume. On a macroscopic scale, network defects decrease stiffness and strength, increase swelling, and decrease chemical stability. To minimize heterogeneity in step-growth hydrogel networks, telechelic prepolymers with defined molar masses and degrees of functionality, like the starPEGs used in this work, are used. This narrowly defined geometry disfavors the formation of back-biting loop structures and renders more homogeneous hydrogels compared to those obtained from polymeric precursors with higher dispersities and less regular geometries.<sup>[19]</sup>

The internal structure and the properties of hydrogel networks are influenced by many factors including the polymer fraction, reactive group concentration, and the molar mass, architecture, length, and backbone composition of crosslinkers. The conversion and the kinetics of the crosslinking reaction, which are a function of pH in thiol-based nucleophilic crosslinking systems like thiol-MS, also influence the crosslinking degree and homogeneity of the network and impact the mechanical properties of the resulting hydrogel. In this work, we study the crosslinking kinetics and mechanical properties of PEG-4TzMS hydrogels formed at controlled pH values as a function of multifunctional thiol crosslinker structure and the degree of functionality varied by prefunctionalization with a bioactive ligand. For all experiments, we selected precursor compositions common in 3D cell culture with the aim of illustrating how typical changes in

compositional parameters can affect the properties of the resulting encapsulation matrix.

The crosslinking degree in a starPEG network is a function of the overall polymer concentration, the rate and efficiency of the crosslinking reaction, and the reactive partner stoichiometry. The impact of the overall polymer content on the properties in step-growth starPEG networks has been studied in depth by other authors.<sup>[20–22]</sup> At concentrations close to the so-called overlap concentrations, the end groups of neighboring starPEG molecules are essentially touching, and the starPEG molecules exhibit an ordered packing arrangement throughout the volume. Covalent connection of the end groups via complementary reactive partners or short crosslinkers is spatially possible and leads to homogeneous gel networks. At concentrations significantly below the overlap concentration, short crosslinkers cannot link the star polymers efficiently, and at significantly higher concentrations the arm chains can entangle. Both cases give rise to network defects such as dangling chains or loops. For a 16 kDa PEG-4VS, the overlap concentration was reported to be 4.0% w/v as determined by dynamic light scattering (DLS) in PBS.<sup>[23]</sup> The hydrogels in the present work were prepared at a constant total polymer concentration of 5% w/v. In **R1** and **R2**, the reactive partners are both 20 kDa starPEGs, meaning the total starPEG concentrations slightly surpass the overlap concentration to facilitate efficient crosslinking. In the systems using linear crosslinkers, starPEG concentration varied from 2.4% w/v when combined with 10 kDa PEG-dithiol (**R3**) to  $\approx 4.5\%$  w/v when combined with the short linear crosslinkers 1 kDa PEG-dithiol or 1.7 kDa VPM (**R4–R6**). These starPEG concentrations straddle the overlap concentration, and were expected to allow efficient crosslinking when combined with the different length linear crosslinkers. Fixing the overall polymer content at 5% w/v, which has been applied for 3D cell encapsulations by us and others,<sup>[3,5,6]</sup> should therefore give favorable compositions for obtaining fully crosslinked networks.

For step-growth crosslinking systems, network homogeneity is maximized under reaction-limited conditions, which allow complete mixing of the reactive partners before appreciable crosslinking has occurred as opposed to diffusion-limited conditions that lock reactive groups in the growing network at non-stoichiometric ratios to generate network inhomogeneities. Crosslinking reactions with pH-adjustable kinetics can offer reaction-controlled crosslinking and gelation on the minutes timescale within certain pH windows. Thiol-based Michael-type addition reactions are widely used in the 3D cell encapsulation community for this purpose, because such reaction kinetics are attainable within certain pH ranges by modulating the concentration of reactive species. Thiol-Mal crosslinking is notoriously rapid and typically generates inhomogeneous networks at physiological pH, but more homogeneous networks at pH values below 7 or by other strategies such as decreasing the concentration of available Mal groups through complexation.<sup>[7]</sup> Thiol-VS crosslinking is slow and requires higher pH values to gel within desired timescales. In our previous work, thiol-MS showed gelation on a minutes time scale at near-physiological pH values. Under these conditions, thiol-MS hydrogels form more homogeneous networks than thiol-Mal and avoid the cell sedimentation during gel formation observed for thiol-VS.<sup>[3]</sup> For TzMS, the second-order rate coefficient ( $17 \text{ M}^{-1} \text{ s}^{-1}$  at pH 7.5)<sup>[24]</sup> is sim-

ilar to that reported for reaction-limited starPEG gelation systems exhibiting high homogeneity.<sup>[25]</sup> In the present work, we refined the buffering conditions to mitigate the effect of released methanesulfinic acid byproduct and maintain a stable pH during crosslinking. The selected buffer, comprising of 20 mM HEPES and 40 mM sodium carbonate, is based on common cell culture conditions,<sup>[11]</sup> and provided excellent pH maintenance for the reactive group concentrations up to 8 mM used in our systems. The enhanced buffering capacity allowed the crosslinking reactions to reach higher conversions, exemplified by system **R2** reaching  $G' = 5.6 \text{ kPa}$  versus **R1** reaching 0.65 kPa at pH 7.0. Methanesulfinic acid was shown to not impact cell viability in previous work,<sup>[3]</sup> and the cytocompatible buffer adopted in the present work now resolves the question<sup>[26]</sup> of how it may influence pH and crosslinking degree.

Gelation kinetics and mechanical properties are affected by changes in functionality, concentration or molar mass of reacting species, an issue typically disregarded despite its importance to reproducible 3D cell encapsulation outcomes.<sup>[3,7]</sup> Overall, we see that gelation time and final stiffness of gels crosslinked with star or linear PEG crosslinkers in this work correlate with the concentration of starPEG in the precursor mixture, which determines the density of network points. The concentration of network points decreases in the order **R2** > **R4** > **R3**. The  $t_{50\text{Pa}}$  values increase, and the  $G'_{40\text{min}}$  values decrease correspondingly. Changing the architecture and molar mass of PEG-based thiol crosslinkers therefore provides a convenient means of tuning the crosslinking rate and final stiffness of hydrogels at fixed overall polymer content and crosslinking conditions. To impart the degradability necessary for cell proliferation, MMP-degradable peptide VPM is a common dithiol-bearing degradable peptide used in 3D cell culture,<sup>[12,13,27,28]</sup> and served as a representative degradable crosslinker for comparison with the PEG crosslinkers in this work. Our work highlights important differences in crosslinking hydrogels with 1 kDa PEG-dithiol (**R4**) and VPM crosslinker (**R5**). Although  $t_{50\text{Pa}}$  values were almost identical in both systems,  $G'_{40\text{min}}$  values were threefold lower (0.8–1.1 kPa) in VPM crosslinked hydrogels. The starPEG and reactive end group concentrations were slightly lower in the VPM hydrogel due to the higher molar mass of VPM (1.7 kDa), but the density of network points was similar in both systems and, therefore, the differences in  $G'_{40\text{min}}$  cannot be completely explained by starPEG concentration and crosslinker length. Mass spectrometry studies highlighted a significant loss of thiol functions through disulfide formation (i.e., thiol coupling) in VPM solutions. This loss could be compensated by adding excess VPM to the formulation without affecting the crosslinking ability of the system. This can be a pragmatic solution to obtain VPM-crosslinked thiol-TzMS hydrogels with higher stiffness for cell culture. Other important features observed in RGD-functionalized and enzymatically-degradable thiol-TzMS PEG hydrogels (**R6**) were that the values for  $t_{50\text{Pa}}$  ranged from just under 1 min at pH 8.0 to 4 min at pH 7.5 and 6 min at pH 7.0, and that the  $G'_{40\text{min}}$  values were in the 240–320 Pa range. These timescales allow comfortable handling and mixing of precursor and cellular components around physiological pH, and the achieved stiffnesses are suitable for 3D cell culture.<sup>[4]</sup> Although this work has focused on the thiol-TzMS crosslinking system, some of the observed features have positive practical implications for other thiol-based nucle-



ophilic crosslinking systems and step-growth hydrogels more broadly.

## 4. Conclusion

Thiol/PEG-4TzMS hydrogels at compositions typically used for 3D cell culture allow comfortable handling during the experimental procedure. We previously demonstrated high cytocompatibility and >2 week gel longevity for fibroblast encapsulation in thiol/PEG-4TzMS gels, without exploring how composition influences the kinetics and mechanics of gel formation that are important for practical implementation of the system. The present work provides details on the expected gelation kinetics and mechanical stability of such networks, and how these vary with changes in the hydrogel formulation that are typically needed to match network properties such as stiffness and degradability with cellular requirements. Buffer containing 20 mM HEPES and 40 mM sodium bicarbonate satisfactorily maintained stable pH values throughout gelation in all systems, negating the effects of released methanesulfinic acid. This pH stability is important for controlling the gelation kinetics, and places the thiol-MS crosslinking alongside other thiol-based nucleophilic crosslinking reactions in which pH also remains stable during crosslinking. We obtained a gelation time of  $\approx 4$  min for the most biologically relevant system that was pre-functionalized with cell-adhesive ligand and crosslinked with degradable peptide VPM at pH 7.5. This timescale is very appealing for 3D cell encapsulation under near-physiological conditions to facilitate complete mixing and homogeneous cell distributions. The relatively low  $G'$  of  $\approx 300$  Pa is suitable for many 3D hydrogel applications, and could be increased to >1 kPa by introducing an excess of VPM crosslinker. Disulfide formation in the VPM system was identified as a contributing factor to lower stiffness values, which is relevant to many hydrogel systems that employ this peptide as crosslinker. We envisage that the properties of the thiol-crosslinked PEG-4TzMS system could be advantageous for automation of 3D cell cultures, where gelation kinetics are well adapted for the timescales of typical mixing protocols in pipetting robots.

## 5. Experimental Section

**Materials:** PEG-4SH (20 kDa) was purchased from JenKem Technologies (Texas, USA). PEG-dithiols (10 and 1 kDa) were bought from Creative PEGworks (North Carolina, USA), and VPM was purchased from GeneCust (France). Buffers were freshly prepared before each rheology experiment by dissolving HEPES and sodium bicarbonate from Sigma-Aldrich (Germany) in Milli-Q water and adjusting the pH value to the target (8.0, 7.5, and 7.0) using 1 M NaOH from Alfa Aesar (Massachusetts, USA). Solvents for  $^1\text{H}$  NMR spectroscopy were purchased from Deutero (Germany). PEG-4TzMS (20 kDa) was synthesized following the previously established protocol.<sup>[4]</sup>

**Equipment:** pH measurements were performed with a Eutech Elite pH Spear (Thermo Scientific). Nuclear magnetic resonance (NMR) spectroscopy was performed with a Bruker Avance 300 MHz equipped with a He cooled 5 mm TCI-CryoProbe (a proton-optimized triple resonance NMR “inverse” probe with external water-cooling unit (CP TCI 500S2, H-C/N-D-05 Z) from Bruker (Massachusetts, USA). All measurements were done at 298 K. The chemical shifts were recorded in parts per million ( $\delta$  ppm) with the NMR solvent peak used as reference. Spectra were analyzed using Bruker's TopSpin software. Analytical high-performance liquid chro-

matography (HPLC) was performed with a JASCO 4000 (Japan) equipped with a Reprisil C18 column (250  $\times$  5 mm) and a UV/Vis detector. A gradient elution profile using Solvent A (water + 0.1% v/v TFA) and Solvent B (ACN/water 95:5 v/v + 0.1% v/v TFA) was employed over 40 min at 1 mL min<sup>-1</sup>, going from 5% to 95% v/v Solvent B. Rheology was performed on a Discovery HR-3 rheometer (TA Instruments, USA) using 12 mm parallel plates and a Peltier stage temperature control system. Measurements were performed with  $T = 25$  °C, gap = 300  $\mu\text{m}$ , strain = 1%, and frequency = 1 Hz. Mass spectrometry was performed with a 6545 Accurate-Mass Quadrupole Time-of-Flight (LC/Q-TOF-MS) with electrospray ionization from Agilent (California, USA). Aliquots of 1.0  $\mu\text{L}$  of sample were autoinjected into the LC system that contains a Poroshell HPH-C18 column (3.0 mm  $\times$  50 mm, 2.7  $\mu\text{m}$ ) and a guard column (3.0 mm  $\times$  5 mm, 2.7  $\mu\text{m}$ ) with column temperature set to 45 °C. The mobile phase consisted of two component solutions: A) water + 0.1% v/v formic acid and B) acetonitrile (ACN) + 0.1% v/v formic acid at a flow rate of 500  $\mu\text{L}$  min<sup>-1</sup>. The eluant composition over time was as follows: 0–0.5 min: 5% B; 0.5–5.5 min: 5–50% B; 5.5–7 min: 50–5% B, 7–12 min 5% B at increased flowrate of 2.0 mL min<sup>-1</sup> for column washing; 12–13 min 5% B at reduced flowrate of 500  $\mu\text{L}$  min<sup>-1</sup> ready for the next sample. After separation, the LC flow entered the dual Agilent Jet Stream (AJS) ESI source set to 3,500 V as capillary voltage, 40 psi nebulizer gas pressure, and 7 L min<sup>-1</sup> dry gas flow, and 300 °C dry gas temperature. The TOF parameters used were an extended dynamic range (2 GHz), 140 V fragmentor voltage, and 45 V skimmer voltage. The mass spectra were acquired in the time interval of 1–5 min in full scan mode in the range of 200–1,700 m/z and with a spectra rate of 4 s<sup>-1</sup>. To determine the formation of S–S bonds, the triply charged adduct of VPM (m/z 566.243), the linear dimeric VPM with loss of 2H, i.e., containing 1 S–S bond (m/z 565.905) and cyclic VPM (unimeric or dimeric, both with m/z 565.571 m/z) were extracted and automatically integrated using Mass Hunter software.

**Quantification of the Degree of Functionality and Molar Mass of Starting Materials:** The degrees of functionalization for the NHS-, TzMS-, RGD-, and SH-terminated PEGs were abbreviated  $F_{\text{NHS}}$ ,  $F_{\text{TzMS}}$ ,  $F_{\text{RGD}}$ ,  $F_{\text{SH}}$  throughout the manuscript. The  $F_{\text{TzMS}}$  was quantified by  $^1\text{H}$ -NMR spectroscopy (Figure S1, Supporting Information) using the spectrum of the precursor PEG-4NHS and its reported  $F_{\text{NHS}}$  (from the supplier) as references. The molar masses of the thiol-bearing PEGs were determined in a similar manner (Figure S2, Supporting Information). See the captions of these figures for details of the calculations.

**Functionalization of PEG-4TzMS with c[RGDFC] Peptide:** A stock solution of PEG-4TzMS ( $F_{\text{TzMS}} = 0.964$ ,  $M_n = 22.2$  kDa) was prepared by dissolving the polymer (16.59 mg,  $7.46 \times 10^{-7}$  mol polymer) in freshly prepared Buffer 2 (171.3  $\mu\text{L}$ ) at pH 8.0. The solution was vortexed for 30 s to fully dissolve the polymer. A stock solution of c[RGDFC] was prepared by dissolving the peptide (0.98 mg,  $1.69 \times 10^{-6}$  mol) in Buffer 2 (280  $\mu\text{L}$ ) at pH 8.0. An aliquot of the c[RGDFC] stock (78.7  $\mu\text{L}$ ,  $4.74 \times 10^{-4}$  mmol, 0.16 equiv. relative to TzMS, targeting  $F_{\text{TzMS}} = 0.80$  after reaction) was added to the stock solution of PEG-4TzMS (39.2  $\mu\text{L}$ ) in an Eppendorf tube at room temperature, vortexed for 30 s, then allowed to react for 60 min, reaching a final pH of 8.06. For purification, the pH was decreased to pH 5 using 1 M HCl, and the solution was dialyzed against water and freeze dried. The  $F_{\text{TzMS}}$  and  $F_{\text{RGD}}$  were determined by  $^1\text{H}$  NMR spectroscopy, with the doublet at 7.6 ppm corresponding to the aromatic protons nearest to the unreacted TzMS units (Figure 2, signal b) and the doublet at 7.5 ppm corresponding to the aromatic protons after replacement of MS with RGD.

**Simulating the Distribution of Functional Species in PEG-4TzMS:** The distribution of stars bearing 0, 1, 2, 3, and 4 functional chain ends was derived for PEG-4TzMS ( $F_{\text{TzMS}} = 0.964$ ) and its RGD-functionalized derivative ( $F_{\text{TzMS}} = 0.833$ ) by Python simulations using the NumPy library (1.23).<sup>[29]</sup> Since kinetics do not affect the distributions and functionalization steps can be treated as subsequent events, the distributions are directly related to the probability of the individual arms in each system being attacked by a reaction partner. There are two limiting cases that define the bounds of this process: 100% diffusion control, in which all star molecules react with the same probability independent of the number of active arms they bear, and 100% chemical control, in which all active arms react with the same probability no matter the star to which they are attached.<sup>[30]</sup>

For both distributions, the functionalization process was simulated according to all possible limiting pathways for systems with 200 000 macromolecules reacting with the reaction partner until the target stoichiometry was reached. In each step, an arm was selected for reaction. In the diffusion control case, a random macromolecular star was selected with equal probability, and in the chemical control case, the probability to be selected was equal for all arms in the system, making molecules with more active arms more likely to react. The  $F_{TzMS} = 0.964$  was assumed to be reached through a functionalization process (i.e., starting from zero functionality, as would be expected in the synthesis of the commercial precursor PEG-4NHS). The  $F_{MS} = 0.833$  system was then deduced through defunctionalization starting from the two limiting cases for the  $F_{TzMS} = 0.964$  system. Average values were calculated from 100 000 sets of simulations. The values in this paper are precise in the reported significant figures.

**Rheological Characterization of Hydrogel Crosslinking:** First, the masses of PEG-4TzMS and crosslinker required in each experiment were determined from Equation 3 (see Supporting Information), which ensures that the overall polymer content is 5.0% w/v and the SH:MS ratio is 1.00. The concentration of the stock solutions of PEG-4TzMS and crosslinker were then determined by imposing equal volumes to facilitate mixing on the rheometer plate. The protocols from the **R2** and **R6** systems at pH 8.0 as representative examples were described here in full. For **R2** (initial pH 8.0), a stock solution of PEG-4TzMS ( $F_{TzMS} = 0.964$ ,  $M_n = 22.2$  kDa) was prepared by dissolving the polymer (10.34 mg,  $4.65 \times 10^{-7}$  mol polymer) in freshly prepared buffer (193.8  $\mu$ L) containing 20 mM HEPES and 40 mM  $\text{NaHCO}_3$  (called Buffer 2) and set to pH 7.7–7.8. The initial pH of this and all other stock solutions for the rheology experiments was pre-determined experimentally to give the target initial pH  $\pm 0.1$  units after dissolving each compound, and are summarized in Table S2 (Supporting Information). The PEG-4TzMS solution was vortexed for 30 s to fully dissolve the polymer. A stock solution of PEG-4SH ( $F_{SH} = 0.914$ ,  $M_n = 20.4$  kDa) was prepared similarly by dissolving the polymer (11.67 mg,  $5.71 \times 10^{-7}$  mol polymer) in freshly prepared buffer (225.2  $\mu$ L) adjusted to pH 7.9. Rheology was then performed within 10 min after solution preparation. An aliquot of PEG-4TzMS solution (18.0  $\mu$ L) was pipetted onto the bottom plate, followed by addition of the PEG-4SH solution (18.0  $\mu$ L) directly into the first drop using a fresh pipette tip. The solution was mixed thoroughly by pipetting up and down for  $\approx 20$  s directly on the plate. The upper plate was lowered to a gap of 300  $\mu$ m, silicone oil was added around the sample to avoid evaporation, and a purge gas cover was placed to avoid disturbance during measurement. The total time required for sample loading until the start of the measurement was 60 s, and measurements were conducted for 40 min. The linear cross-linked systems **R3–R5** were prepared similarly. Note that the pH of the buffer needed to be significantly raised when dissolving VPM (**R5**), in order to reach the target initial pH values before rheology (see Table S2, Supporting Information). The **R1** systems used 10 mM HEPES (Buffer 1) at the target initial pH value prior to dissolving the solids, and was otherwise identical to **R2**. For **R6**, functionalization of PEG-4TzMS with c[RGDfC] was performed identically to described above, up to the purification step. After the 60 min reaction time, a final pH of 8.06 was reached. Note that the pH 7.5 and 7.0 systems required the addition of 1 M HCl (2.5 and 5.0  $\mu$ L, respectively) to attain the targeted initial pH value. Additional Buffer 2 (39.1, 36.7, or 34.1  $\mu$ L for pH 8.0, 7.5, and 7.0 systems, respectively) at the target pH value was added to make up the required volume. As crosslinker, VPM peptide (1.36 mg,  $8.01 \times 10^{-7}$  mol) was dissolved in Buffer 2 (124.5  $\mu$ L) pre-adjusted to initial pH of 9.93, 9.41, or 9.01 (for pH 8.0, 7.5, and 7.0 systems, respectively) and rheology was performed by adding the two solutions to the rheometer as described for **R2**.

**pH Tracking During Hydrogel Formation:** For each composition described in Table 1, a solution of the thiol component (80  $\mu$ L) was added to a solution of the PEG-4TzMS component (80  $\mu$ L) in an Eppendorf tube. The stock solutions were prepared with identical concentrations to in the rheology experiments. After vortexing for 30 s, the pH-meter probe was introduced into the solution and the Eppendorf tube with the probe inside was sealed with Parafilm. Values for pH were manually recorded over 40 min.

## Supporting Information

Supporting Information is available from the Wiley Online Library or from the author.

## Acknowledgements

S.P. and A.D.C. received funding from the European Union's Horizon 2020 research and innovation program under the FET PROACTIVE grant agreement no. 731957 (Mechano-Control) and the Senatsausschuss Wettbewerb (SAW) Leibniz-Transfer program under project uTissueFab. J.I.P. received funding from the Deutsche Forschungsgemeinschaft (DFG, project no. 422041745).

Open access funding enabled and organized by Projekt DEAL.

## Conflict of Interest

The authors declare no conflict of interest.

## Data Availability Statement

The data that support the findings of this study are available from the corresponding author upon reasonable request.

## Keywords

cell culture, cell encapsulation, crosslinking, gelation, hydrogel

Received: October 5, 2022

Revised: November 17, 2022

Published online: December 11, 2022

- [1] S. Correa, A. K. Grosskopf, H. Lopez Hernandez, D. Chan, A. C. Yu, L. M. Stapleton, E. A. Appel, *Chem. Rev.* **2021**, *121*, 11385.
- [2] L. G. Griffith, M. A. Swartz, *Nat. Rev. Mol. Cell Biol.* **2006**, *7*, 211.
- [3] J. I. Paez, A. Farrukh, R. Valbuena-Mendoza, M. K. Włodarczyk-Biegun, A. Del Campo, *ACS Appl. Mater. Interfaces* **2020**, *12*, 8062.
- [4] J. I. Paez, A. De Miguel-Jiménez, R. Valbuena-Mendoza, A. Rathore, M. Jin, A. Gläser, S. Pearson, A. Del Campo, *Biomacromolecules* **2021**, *22*, 2874.
- [5] E. A. Phelps, N. O. Enemchukwu, V. F. Fiore, J. C. Sy, N. Murthy, T. A. Sulchek, T. H. Barker, A. J. García, *Adv. Mater.* **2012**, *24*, 64.
- [6] J. Kim, Y. P. Kong, S. M. Niedzielski, R. K. Singh, A. J. Putnam, A. Shikanov, *Soft Matter* **2016**, *12*, 2076.
- [7] B. Xue, D. Tang, X. Wu, Z. Xu, J. Gu, Y. Han, Z. Zhu, M. Qin, X. Zou, W. Wang, Y. Cao, *Proc. Natl. Acad. Sci. USA* **2021**, *118*, e2110961118.
- [8] M. Mours, H. H. Winter, *Macromolecules* **1996**, *29*, 7221.
- [9] M. Kurakazu, T. Katashima, M. Chijiishi, K. Nishi, Y. Akagi, T. Matsunaga, M. Shibayama, U.-I. Chung, T. Sakai, *Macromolecules* **2010**, *43*, 3935.
- [10] N. E. Good, G. D. Winget, W. Winter, T. N. Connolly, S. Izawa, R. M. M. Singh, *Biochemistry* **1966**, *5*, 467.
- [11] J. Michl, K. C. Park, P. Swietach, *Commun. Biol.* **2019**, *2*, 144.
- [12] M. P. Lutolf, J. L. Lauer-Fields, H. G. Schmoekel, A. T. Metters, F. E. Weber, G. B. Fields, J. A. Hubbell, *Proc. Natl. Acad. Sci. USA* **2003**, *100*, 5413.
- [13] J. Patterson, J. A. Hubbell, *Biomaterials* **2010**, *31*, 7836.
- [14] L. M. Weber, K. N. Hayda, K. Haskins, K. S. Anseth, *Biomaterials* **2007**, *28*, 3004.

- [15] M. J. O'melia, A. Mulero-Russe, J. Kim, A. Pybus, D. Deryckere, L. Wood, D. K. Graham, E. Botchwey, A. J. García, S. N. Thomas, *Adv. Mater.* **2022**, *34*, 2108084.
- [16] C. A. Deforest, E. A. Sims, K. S. Anseth, *Chem. Mater.* **2010**, *22*, 4783.
- [17] C. M. Madl, B. L. Lesavage, R. E. Dewi, C. B. Dinh, R. S. Stowers, M. Khariton, K. J. Lampe, D. Nguyen, O. Chaudhuri, A. Enejder, S. C. Heilshorn, *Nat. Mater.* **2017**, *16*, 1233.
- [18] T. Sakai, *Polym. J.* **2014**, *46*, 517.
- [19] Y. Akagi, T. Matsunaga, M. Shibayama, U.-I. Chung, T. Sakai, *Macromolecules* **2010**, *43*, 488.
- [20] W. Liu, X. Gong, Y. Zhu, J. Wang, T. Ngai, C. Wu, *Macromolecules* **2019**, *52*, 8956.
- [21] X. Li, S. Nakagawa, Y. Tsuji, N. Watanabe, M. Shibayama, *Sci. Adv.* **2019**, *5*, eaax8647.
- [22] M. Tosa, K. Hashimoto, H. Kokubo, K. Ueno, M. Watanabe, *Soft Matter* **2020**, *16*, 4290.
- [23] J. Wang, F. Zhang, W. P. Tsang, C. Wan, C. Wu, *Biomaterials* **2017**, *120*, 11.
- [24] X. Chen, H. Wu, C.-M. Park, T. H. Poole, G. Keceli, N. O. Devarie-Baez, A. W. Tsang, W. T. Lowther, L. B. Poole, S. B. King, M. Xian, C. M. Furdui, *ACS Chem. Biol.* **2017**, *12*, 2201.
- [25] K. Nishi, K. Fujii, Y. Katsumoto, T. Sakai, M. Shibayama, *Macromolecules* **2014**, *47*, 3274.
- [26] Y. Gao, K. Peng, S. Mitragotri, *Adv. Mater.* **2021**, *33*, 2006362.
- [27] M. D. Hunckler, J. D. Medina, M. M. Coronel, J. D. Weaver, C. L. Stabler, A. J. García, *Adv. Healthcare Mater.* **2019**, *8*, 1900371.
- [28] A. Farrukh, J. I. Paez, A. Del Campo, *Adv. Funct. Mater.* **2019**, *29*, 1807734.
- [29] C. R. Harris, K. J. Millman, S. J. Van Der Walt, R. Gommers, P. Virtanen, D. Cournapeau, E. Wieser, J. Taylor, S. Berg, N. J. Smith, R. Kern, M. Picus, S. Hoyer, M. H. Van Kerkwijk, M. Brett, A. Haldane, J. F. Del Río, M. Wiebe, P. Peterson, P. Gérard-Marchant, K. Sheppard, T. Reddy, W. Weckesser, H. Abbasi, C. Gohlke, T. E. Oliphant, *Nature* **2020**, *585*, 357.
- [30] B. Ebeling, M. Eggers, P. Vana, *Macromolecules* **2010**, *43*, 10283.